The rotation of solid cylinders in transverse magnetic fields

1982 J. Phys. A: Math. Gen. 15 1689

(http://iopscience.iop.org/0305-4470/15/5/029)

J. Phys. A: Math. Gen. **15** (1982) 1689–1700. Printed in Great Britain

The rotation of solid cylinders in transverse magnetic fields

R S Peckover
UKAEA, Culham Laboratory, Abingdon, Oxon. OX14 3DB, England

Received 22 September 1981

Abstract. A cylinder driven to rotate against friction in a uniform transverse magnetic field is considered both when the field is constrained to pass through the cylinder and *in vacuo* when it may be expelled. The rotation rate is reduced as the field strength is increased. Whereas *in vacuo* the transition between high and low rotation rates is accomplished by means of a catastrophic jump, the transition in the constrained flux case is smooth, and is similar to that for convection in a fluid layer in the presence of a vertical magnetic field. A simple relationship between the RMS magnetic field and the peak field is presented, involving the 'magnetic flux number' $\mathcal{H}$.

1. Introduction

When an electrically conducting cylinder of solid material is made to rotate against friction in a transverse magnetic field *in vacuo*, a range of conditions exists for which there is more than one stable steady rotation rate (Gimblett and Peckover 1979, Peckover and Gimblett 1981). The system is an example of Thom's cusp catastrophe (Thom 1975). Small changes in the control parameters result in substantial changes in the rotation rate, and in the magnetic field configuration within the cylinder. By contrast, a closely related configuration with a fixed flux boundary condition (analysed in this paper) has no catastrophic behaviour. It is concluded that the magnetic flux number $\mathcal{H}$ is a key parameter, in terms of which a simple relation between the peak magnetic field B^* and the RMS field $\bar{B}$ within the cylinder is presented.

The equations appropriate for rotating cyclinders are given in the next section. The constant flux model is analysed in § 3, and the salient features of the *in vacuo* solution recalled in § 4. The $\bar{B} - B^*$ relation is obtained in § 5. Finally the differences and similarities between these two configurations are discussed.

This system provides a simple example of the dynamic interaction between a magnetic field and moving electrically conducting material. Much of the early work on induction in solid rotators was motivated by problems in geomagnetism, in particular the problem of the origin of the Earth's magnetic field. The electromagnetic generation of centrifugal flow by applying rotating fields to cylinders containing liquid metals has some features in common with this system. The rotation of convective eddies in the sun is responsible for the concentration of magnetic fields into flux ropes at the solar photosphere. References to these related topics are to be found in the first two papers cited above.

0305-4470/82/051689+12$02.00

2. Configuration and equations

Consider a long right circular solid cylinder of mass M, length L, and radius $a(\ll L)$, rotating about its principal axis, which to be specific is taken as horizontal. The rotation takes place in a transverse (vertical) applied magnetic field of uniform strength B_0. End effects are neglected and the configuration may be considered to be essentially two dimensional. The cylinder rotation induces currents parallel to the axis of rotation and hence a magnetic torque $\mathscr{M}$ about that axis. For convenience the current flow is imagined to be closed by a suitably arranged external circuit which interferes in no other way with the system. The rotation is assumed to be driven by a steady applied torque $\mathscr{J}$ and opposed by a frictional torque $\mathscr{L}$ taken to be proportional to the instantaneous rate of rotation.

The angular momentum equation for the cylinder is

$$I(\mathrm{d}\Omega/\mathrm{d}t) = \mathscr{J} - \mathscr{L} - \mathscr{M} \tag{2.1}$$

where $\Omega(t)\hat{Z}$ is the angular velocity using cylindrical coordinates $(\tilde{r}, \theta, Z)$ and $I = \frac{1}{2}Ma^2$; here M is the mass of the cyclinder. Let us express the frictional torque $\mathscr{L}$ which is by hypothesis proportional to the angular velocity Ω as

$$\mathscr{L} = \tfrac{1}{2}\lambda M\Omega \tag{2.2}$$

where λ is a coefficient of friction with dimension $[\mathrm{L}^2\mathrm{T}^{-1}]$. In the absence of a magnetic field, a steady angular velocity Ω_0 will be attained in which the driving torque balances friction; hence $\mathscr{J} = \frac{1}{2}\lambda M\Omega_0$. It is convenient to introduce dimensionless variables $r = \tilde{r}/a$, $U = a^2\Omega/\lambda$ and $\tau = \lambda t/a^2$ where a^2/λ is a 'friction' time scale. The equation for the angular momentum for the cylinder can thus be written in non-dimensional form as

$$\mathrm{d}U/\mathrm{d}\tau = U_0 - U - \mathscr{M}^*. \tag{2.3}$$

If B_0 is the dimensionless measure of the ambient magnetic field, being the ratio of the Alfven speed to the friction speed λ/a, then the dimensionless flux function α can be defined by $\boldsymbol{B} = B_0\mathrm{curl}\,(\alpha\hat{Z})$ and the dimensionless magnetic torque M^* can be expressed as

$$\mathscr{M}^* = \frac{2B_0^2}{\pi}\int r(\partial\alpha/\partial\theta)\nabla^2\alpha\,\mathrm{d}r\,\mathrm{d}\theta. \tag{2.4}$$

The function α satisfies

$$\partial\alpha/\partial\tau + U\partial\alpha/\partial\theta = p_\mathrm{m}^{-1}\nabla^2\alpha \tag{2.5}$$

where p_m is a modified magnetic Prandtl number given by λ/η. Here the uniform and constant magnetic diffusivity η is given by $(\mu\gamma)^{-1}$ where μ and γ are the cylinder permeability and electrical conductivity respectively. The modified Chandrasekhar number Q (see, for example, Weiss (1964)) is defined here as $p_\mathrm{m}B_0^2$, and is a measure of the influence of the magnetic field on the cylinder's rotation rate. The dimensionless angular velocity U is the 'Reynolds number' for the system and the 'magnetic Reynolds number' $R = p_\mathrm{m}U$.

3. Solution for constant flux

When a cylinder rotates *in vacuo*, the magnetic field is increasingly expelled from the cylinder as the rotation rate increases, and in the limit of infinite rotation rate no

magnetic field penetrates into the cylinder. It is intended here to investigate the effect of compelling the flux to penetrate the cylinder, as would occur, for example, if the cylinder were placed in a vertical slot of the same diameter between two vertical perfectly insulating walls. A simple but somewhat idealised boundary condition which ensures the flux does pass through the cylinder is one where the magnetic field is unperturbed outside the cylinder i.e. $\alpha = \cos\theta$ on $r = 1$ (see figure 1). This corresponds

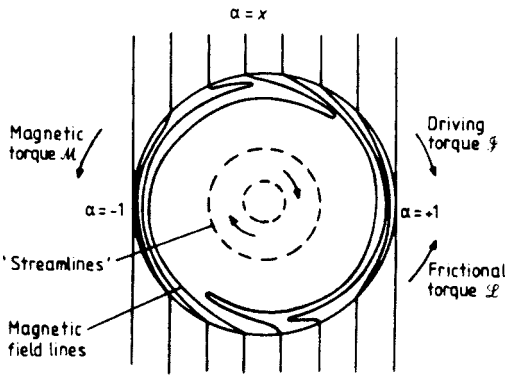

Figure 1. Magnetic field lines for a cylinder rotating in an unperturbed external field, where α is the flux function. The flux number $\mathscr{H}$ is conserved.

to setting the field uniformly in the absence of rotation with the region exterior to the cylinder being a perfect superconductor. With this choice of boundary condition, the time-independent solution of (2.5) is

$$\alpha = \mathrm{Re}\left(\frac{J_1(qr)}{J_1(q)}\,e^{i\theta}\right) \tag{3.1}$$

where $q^2 = -iR$ and J_1 denotes the Bessel function of the first kind and first order. It follows that the magnetic torque is

$$\mathscr{M}^* = \tfrac{1}{2}B_0^2\,\mathrm{Im}(S) \tag{3.2}$$

where $S \equiv qJ_0(q)/J_1(q)$. The complex function S is discussed in the appendix. $\mathrm{Im}(S)$ and hence $\mathscr{M}^*$ is a monotonic function of R.

In equilibrium (2.3) becomes

$$R_0 = R + \tfrac{1}{2}Q\,\mathrm{Im}(S) \tag{3.3}$$

which implicitly gives R as a function of Q for any choice of R_0.

If $\langle X\rangle$ is the average over the cylinder of any quantity X, then the RMS magnetic field $\bar{B}$ is defined by $\bar{B}^2 = \langle B^2\rangle$, and is found to be given by

$$\bar{B}^2 = (\mathrm{Re}(S) - 1)B_0^2. \tag{3.4}$$

Figure 2 shows that $\bar{B}$ is a monotonically increasing function of R.

The magnitude of the magnetic field as $r \to 1$ is given by

$$B_1(\theta) \equiv (\Sigma^2\cos^2(\theta+\beta) + \sin^2\theta)^{1/2}B_0 \tag{3.5}$$

where Σ and β are defined in the appendix. One can show that the peak magnetic

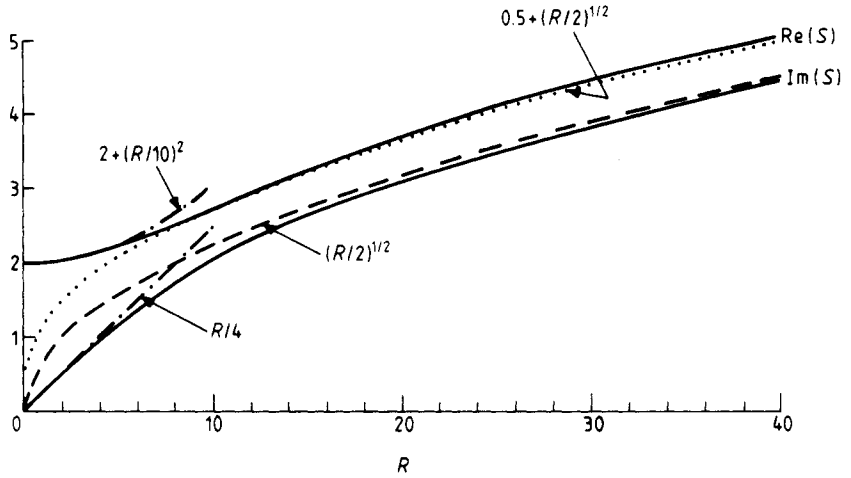

Figure 2. The dependence of Re(S) and Im(S) on R.

field B^* must occur at the periphery; hence

$$B^* = \max_{\theta} (B_1(\theta)). \tag{3.6}$$

Since $B_1(0) = \Sigma \cos \beta = (\mathrm{Re}(S) - 1)$, it follows that

$$B^* \geqslant (\mathrm{Re}(S) - 1) B_0 \tag{3.7}$$

which when combined with (3.4) gives $B^* B_0 \geqslant \bar{B}^2$.

The maximum tangential component of the magnetic field B_θ^* occurs when $\theta = -\beta$, and $B_1(-\beta) = (\Sigma^2 + \sin^2 \beta)^{1/2} B_0$. This provides a reasonable estimate for B^*, but a more accurate value depends on the regime (see below and figure 5).

If an ambient field strength B_0 is chosen, and p_m is given, then (3.3) can be used to calculate the magnetic Reynolds number of the rotating cylinder in equilibrium.

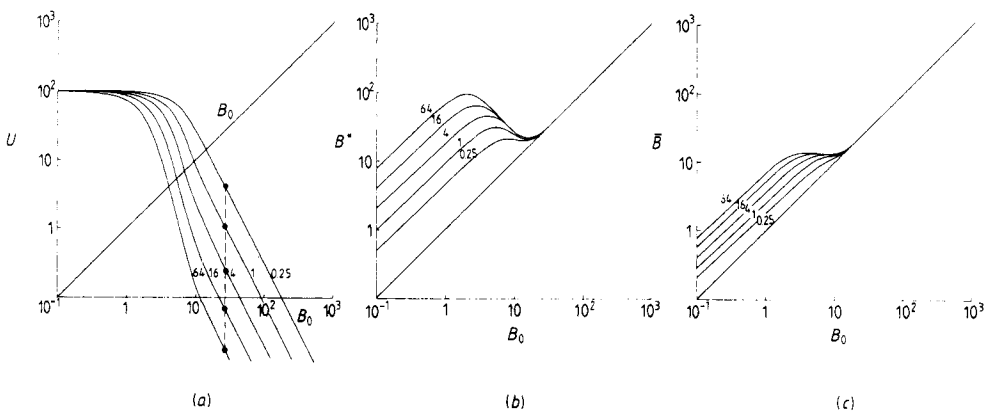

Figure 3. The dependence of (*a*) U, (*b*) B^* and (*c*) $\bar{B}$ on the applied field B_0 for the constant flux rotating cylinder. The curves are labelled with the appropriate value of p_m. In (*a*), the value of U at which $R = 1$ is indicated on each curve.

Equation (3.1) then gives the magnetic field distribution, with (3.4) and (3.6) giving $\bar{B}$ and B^* respectively. Figure 3 shows the rotation speed $U(\equiv R/p_m)$, the peak magnetic field B^* and the RMS magnetic field $\bar{B}$ as functions of the ambient field strength B_0 for different values of p_m. For small p_m only two regimes exist—a 'weak' field and a 'strong' field regime. As p_m increases a third intermediate regime emerges. The three regimes are most clearly distinguishable when p_m is large, and figure 4(*a*) shows the case $p_m = 10^4$. These regimes are here called the 'kinematic', the 'dynamic' and the 'magnetic drag' regimes.

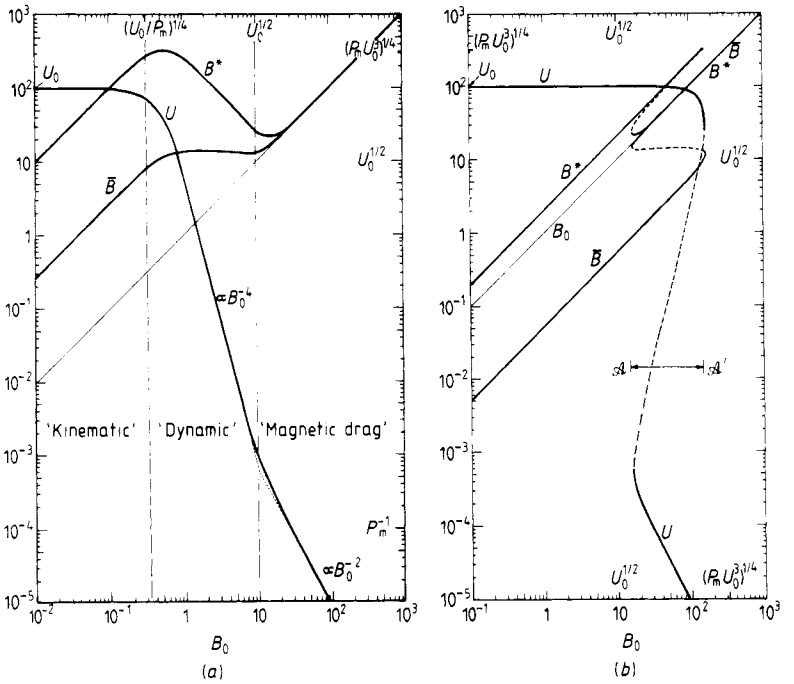

Figure 4. The rotation speed U, the peak B^*, and the RMS field $\bar{B}$ for a solid cylinder rotating in an applied magnetic field B_0 which is (*a*) unperturbed outside the cylinder (*b*) *in vacuo*; $p_m = 10^4$. In (*a*), $B_m \equiv \max(B^*)$ exceeds U_0, and $\bar{B}$ is constant in the dynamic regime $\mathscr{A}\mathscr{A}'$, giving hysteresis. The unstable equilibrium branch is shown by the broken curve.

For both the kinematic and dynamic regimes, R is large. The magnetic field is expelled from the central region and concentrated in a boundary layer of thickness $R^{-1/2}$ at the periphery of the cylinder. Asymptotically for large R

$$\alpha = r^{-1/2} \exp(-G) \sin(\theta + G) \tag{3.8}$$

where $G = (1-r)(\frac{1}{2}R)^{1/2}$; thus the tangential magnetic field at $r = 1$ is given by

$$B_\theta = B_0 R^{1/2} \sin(\theta - \tfrac{1}{4}\pi). \tag{3.9}$$

Figure 5 shows that $\theta = -\frac{1}{4}\pi$ is a good approximation for the location of the maximum tangential field for $R \geqslant 5$. For large R,

$$\bar{B} = (\tfrac{1}{2}R)^{1/4} B_0 \tag{3.10}$$

$$B^* = R^{1/2} B_0 \tag{3.11}$$

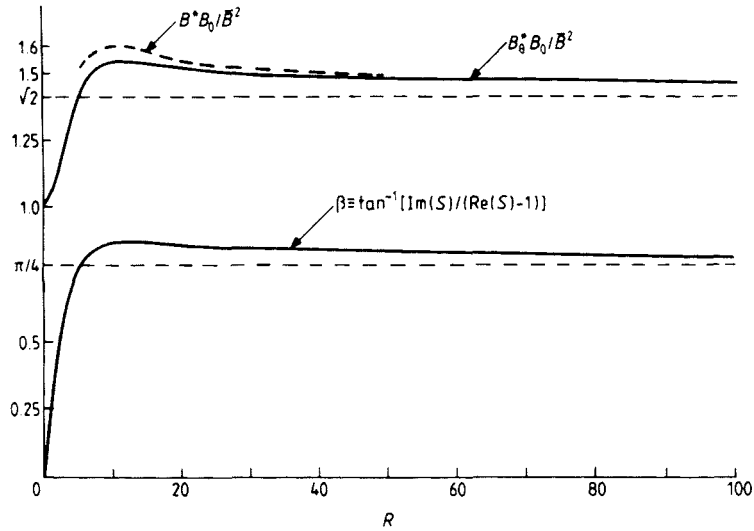

Figure 5. For the constant $\mathscr{H}$ rotating cylinder, β is shown as a function of R; β is the value of θ at which B_θ^* is maximum. The ratios $B_\theta^*B_0/\bar{B}^2$ and $B^*B_0/\bar{B}^2$ ($\equiv \frac{1}{2}\mathscr{P}$) are also shown.

and (3.3) becomes

$$R_0 = R + cQR^{1/2} \tag{3.12}$$

where $c = (2\sqrt{2})^{-1}$ is a constant of order unity. The relative strength of the terms on the RHS of (3.12) distinguishes between the 'kinematic' and 'dynamic' regimes.

If $Q \ll R^{1/2}$, the second term may be neglected. This is the 'kinematic' regime in which the magnetic field has a negligible influence on the rotation rate, which is determined simply by a balance between driving torque and friction. It follows that

$$R = R_0 \qquad \bar{B} = (\tfrac{1}{2}R_0)^{1/4}B_0 \qquad B^* = R_0^{1/2}B_0 \tag{3.13}$$

in the kinematic regime.

If $Q \gg R^{1/2} \gg 1$, then the second term is dominant. This is the 'dynamic' regime in which the magnetic field is important and the rotation rate is determined by a balance between the driving torque and Lorentz forces generated by the skin current in the boundary layer; thus the input power is dissipated ohmically. It follows that

$$R \doteq (R_0/Q)^2 \qquad \bar{B} \doteq U_0^{1/2} \qquad B^* \doteq U_0/B_0 \tag{3.14}$$

in the dynamic regime (where $\doteq$ means that constants of order unity have been ignored). It is noteworthy that the RMS magnetic field is essentially constant in this regime, that the peak field decreases as the applied field is increased, and that the rotation speed U decreases steeply (as ${B_0}^4$) as the applied field is increased.

At the transition between the kinematic and dynamic regimes, the peak field has a maximum B_m as a function of the applied field. Its value is of the order of $(p_m U_0^3)^{1/4}$.

The third, 'magnetic drag', regime corresponds to $R \ll 1$. In this case we have to first order

$$R = R_0/[1 + (Q/8\sqrt{2})] \qquad \bar{B} = B_0 \qquad B^* = B_0. \tag{3.15}$$

The magnetic field permeates the whole cylinder and is only perturbed slightly. The rotation rate is almost completely determined by a balance between the driving torque and the strong magnetic field which exerts a drag with coefficient proportional to Q. In this regime U decreases as B_0^{-2}. The transition between dynamic and magnetic drag regimes occurs when $Q \sim R_0$. The characteristics of the three regimes are summarised in table 1.

Table 1. The values to within a factor of order unity of the magnetic Reynolds number R, the peak Chandrasekhar number $Q^* = p_m B^{*2}$, and the mean Chandrasekhar number $\bar{Q} \equiv p_m \bar{B}^2$ in the three regimes. The transition from I to II is when B^* has its peak value and the transition from II to III corresponds to $R \sim 1$. The values for U, B^* and $\bar{B}$ are also shown.

Regime	R	Q^*	$\bar{Q}$	U	B^*	$\bar{B}$
I Kinematic	R_0	$R_0 Q$	$R_0^{1/2} Q$	U_0	$(p_m U_0)^{1/2} B_0$	$(p_m U_0)^{1/4} B_0$
Peak for B^* $(Q = R_0^{1/2})$	R_0	$(R_0)^{3/2}$	R_0	U_0	$(p_m U_0^3)^{1/4}$	$U_0^{1/2}$
II Dynamic	$(R_0/Q)^2$	R_0^2/Q	R_0	$U_0^2/(p_m B_0^4)$	U_0/B_0	$U_0^{1/2}$
Transition $(Q = R_0)$	1	R_0	R_0	p_m^{-1}	$U_0^{1/2}$	$U_0^{1/2}$
III Magnetic drag	R_0/Q	Q	Q	$U_0/(p_m B_0^2)$	B_0	B_0

4. Solution *in vacuo*

An analysis of a cylinder rotating *in vacuo* was presented and discussed by Gimblett and Peckover (1979) (see also Parker 1966, Moffatt 1978). The key features are recalled here so that comparisons may be made with § 3.

The solution for the flux function can be written as

$$\alpha = \frac{2}{\sigma} \operatorname{Re}\left(\frac{J_1(qr)}{J_1(q)} e^{i(\theta - \phi)} \right) \tag{4.1}$$

where $S \equiv \sigma \exp(i\phi)$, as defined in the appendix. Comparison with (3.1) shows that the *in vacuo* solution is obtained from the constant flux solution of §3 by scaling by a factor of $(2/\sigma)$ and rotating through an angle $-\phi$ which tends to $-\frac{1}{4}\pi$ as $R \to \infty$. It follows that the peak field and RMS field within the cylinder are scaled in the same fashion. For the retarding torque on the cylinder, a quadratic scaling enters. Hence $\operatorname{Im}(S)$ is replaced in (3.3) by $-4 \operatorname{Im}(S^{-1})$, giving

$$R_0 = R - 2Q \operatorname{Im}(S^{-1}). \tag{4.2}$$

When $R \gg 1$, $\operatorname{Im}(S^{-1})$ is equal to $-(2R)^{-1/2}$ which implies that the second term on the right-hand side of (4.2) can be neglected provided $B_0 \ll R_0^{1/4} U_0^{1/2}$. Thus for the kinematic regime

$$R = R_0 \qquad \bar{B} = 2B_0/(2R_0)^{1/4} \qquad B^* = 2B_0. \tag{4.3}$$

The form of $\bar{B}$ shows that the field is completely expelled from the cylinder as $R_0 \to \infty$ (Moffat 1978).

When $R \ll 1$, the magnetic field continues to permeate the whole cylinder and is only slightly perturbed. Thus in this 'magnetic drag' regime

$$R = R_0/(\tfrac{1}{8}Q + 1) \qquad \bar{B} = B_0 \qquad B^* = B_0. \tag{4.4}$$

Figure 4(*b*) shows plots of U, B^* and $\bar{B}$ for $p_m = 10^4$ for the *in vacuo* case, which is to be compared with the analogous constant flux case shown in figure 4(*a*). Gimblett and Peckover (1979) have shown that (4.2) makes R a triple valued function of B_0 for $U_0^{1/2} \leqslant B_0 \leqslant R_0^{1/4} U_0^{1/2}$ when $R_0 \geqslant 40$, and that only the upper 'kinematic' and lower 'magnetic drag' branches correspond to stable equilibrium rotation rates. These overlap with the consequence that the 'dynamic' regime does not exist for the cylinder rotating *in vacuo*, and hysteresis occurs. (Note that this hysteresis is *electro*magnetic, not magnetic; the permeability is taken to be constant in this analysis.) It is interesting to observe in figure 4(*b*) that for the unstable branch $\bar{B} \doteq U_0^{1/2}$ as for the dynamic regime of § 3 (see equation (3.14)); this implies that ohmic and frictional dissipation are comparable. When $R_0 \leqslant 40$, the fold in R is absent and the kinematic regime passes over smoothly into the magnetic drag regime.

5. $\bar{B} - B^*$ relations

In this section relations between $\bar{B}$ and B^* are established for a wider class of configurations than considered so far. Suppose that a vertical magnetic field is applied transversely to a horizontal cylinder whose cross section is of area $\mathscr{D}$ with bounding curve ℓ which is of non-negative curvature and which does not rotate. Any incompressible two-dimensional motions are permitted within this envelope subject only to ℓ being a streamline. Obviously a rotating circular cylinder is a special case of this class of configuration with circular streamlines, and a bounding surface shape which is invariant under rotation. Within this cylinder, $B^2 = B_0^2 |\nabla\alpha|^2$ where α is the Z component of the magnetic vector potential. Hence

$$\bar{B}^2/B_0^2 = \langle \alpha j \rangle + \mathscr{D}^{-1} \oint_\ell \alpha \frac{\partial \alpha}{\partial n} \, \mathrm{d}s \tag{5.1}$$

where $j \equiv -\nabla^2\alpha$ is the electric current density. Now for steady motions in two dimensions, the magnetic flux equation is $p_m(\boldsymbol{u} \cdot \nabla)\alpha = \nabla^2\alpha = -j$ where $\boldsymbol{u}$ is the velocity and is a function of position (see Peckover and Weiss (1978) for a detailed derivation). It follows that $\langle \alpha \cdot j \rangle$ vanishes since the curve ℓ is a streamline, and the right-hand side of (5.1) reduces to a single term.

It is convenient to introduce the quantity $\mathscr{H}$ defined by

$$\mathscr{H} = \oint_\ell |\boldsymbol{B}_n| \, \mathrm{d}s. \tag{5.2}$$

Then $\mathscr{H}$, the 'magnetic flux number', is equal to the total number of intersections of lines of force with ℓ (Hide 1978, 1979). Since each field line must enter and leave the cylinder an equal number of times, $\mathscr{H}$ is the sum of the flux entering and the flux leaving the cylinder and these two contributions are equal. $\mathscr{H}$ can also be written as $\oint |\partial\alpha/\partial s| \, \mathrm{d}s$ where α is the dimensionless vector potential. Now since ℓ is a closed curve, α is a periodic function when measured along ℓ. Since α is only defined up to an additive constant, the latter may be chosen so that the maximum value of α is α_0 and its minimum value is $-\alpha_0$. If the curve ℓ can be divided into only two segments ℓ^+ and ℓ^- on one of which the magnetic field vectors are directed into $\mathscr{D}$ and on the other are directed outwards, then $\mathscr{H} = 4\alpha_0 B_0$. If there are more alternating segments,

then it is easy to see that $\mathscr{H} > 4\alpha_0 B_0$. Since every field line must enter and leave at least once it is clear that $\mathscr{H} \geqslant 4\alpha_0 B_0$ in general.

With the definition of α such that $-\alpha_0 \leqslant \alpha \leqslant \alpha_0$ then $|\alpha| \leqslant \alpha_0 \leqslant \mathscr{H}/4B_0$. Moreover $B_0|\partial\alpha/\partial n|$ cannot exceed at any point the peak field B^* for the region $\mathscr{D}$. Thus since

$$\bar{B}^2 < B_0^2 \mathscr{D}^{-1} \oint_\ell |\alpha| \left|\frac{\partial \alpha}{\partial n}\right| \mathrm{d}s \tag{5.3}$$

it follows that

$$\bar{B}^2 < \mathscr{H} B^* / \bar{D} \tag{5.4}$$

where the hydraulic diameter $\bar{D}$ is $4\mathscr{D}/\oint \mathrm{d}s$ (Prandtl and Tietjens 1974). (For a circular cylinder of radius a, $\bar{D} = 2a$.) If $\mathscr{P} \equiv \mathscr{H} B^*/\bar{D}\bar{B}^2$ then (5.4) implies $\mathscr{P} > 1$, strictly.

For the rotating cylinder with constant flux considered in § 3, $\mathscr{H}$ is a constant equal to $4B_0 a$. When $R \to \infty$, $\mathscr{P} \to 2\sqrt{2}$; when $R \to 0$, $\mathscr{P} \to 2$. Figure 5 shows $B^* B_0/\bar{B}^2$ i.e. $\frac{1}{2}\mathscr{P}$ as a function of R. $\mathscr{P}$ has a maximum value of the order of 3.5 when $R \sim 10$.

For the rotating cylinder *in vacuo*, all of the quantities $\mathscr{H}$, B^* and $\bar{B}$ are multiplied by a factor of $(2/\sigma)$ relative to the constant flux case. Hence $\mathscr{P}$ is the same function of R for a cylinder rotating *in vacuo* as for a constant flux case.

6. Discussion

Solutions are given in § 3 and § 4 for a rotating cylinder: (i) with a constant flux number $\mathscr{H}$, and (ii) *in vacuo*. For any specific value of the magnetic Reynolds number R, the magnetic field within the cylinder is identical in the two cases, but the magnitudes of the fields differ by a factor of $(2/\sigma)$. When R_0 (a measure of the driving torque) is less than about 40, R is a smooth and monotonically decreasing function of the applied field B_0. This is true also for all values of R_0 for the constant $\mathscr{H}$ case. *In vacuo*, however, a fold develops in the equilibrium curve for $R_0 \geqslant 40$, and a range of magnetic Reynolds number $R_0/Q \leqslant R \leqslant R_0$ is inaccessible in equilibrium. This range corresponds to that for the dynamic regime in the constant $\mathscr{H}$ case.

In the kinematic regime, $U \sim U_0$ in both cases. For constant $\mathscr{H}$, both B^* and $\bar{B}$ are substantially amplified (when $R_0 \gg 1$), whereas *in vacuo* $B^* = 2B_0$, and $\bar{B}$ decreases as a result of flux expulsion.

In the magnetic drag regime, B^* and $\bar{B}$ remain close to the applied field B_0 in both cases, and the velocity U decreases as B_0^{-2}.

In the dynamic regime for constant $\mathscr{H}$ the peak field B^* decreases with increasing B_0 as U_0/B_0, the RMS field $\bar{B}$ is constant, equal to about $U_0^{1/2}$, and the velocity decreases very steeply (as B_0^{-4}). In the unstable (and hence non-existent) branch *in vacuo*, $\bar{B}$ is also equal to $U_0^{1/2}$, but U increases as B_0^4 (which is of course physically absurd).

If $\bar{Q}$ is defined to be $p_m \bar{B}^2$, i.e. the modified Chandrasekhar number based on the RMS field in the cylinder, then the angular momentum balance equation (2.3) can be represented in dynamic equilibrium for both systems by the following pair of 'magnetic braking' equations:

$$\begin{aligned} R_0 - R &\doteq \bar{Q} \qquad && R \geqslant 1 \\ R_0 - R &\doteq R\bar{Q} \qquad && R \leqslant 1. \end{aligned} \tag{6.1}$$

For the constant $\mathscr{H}$ case, the maximum peak field $B_m = (p_m/U_0)^{1/4}U_0$. Thus for sufficiently large p_m, $B_m > U_0$. Hence in this configuration B^* is not limited by equipartition arguments which would imply $B^* \leqslant U_0$.

It is of some interest to compare the constant flux number rotating cylinder problem with another constant $\mathscr{H}$ configuration—that of convection in a fluid layer permeated by a vertical magnetic field with insulated side walls which constrains all the magnetic flux to pass through the layer. Such a configuration was considered by Peckover and Weiss (1972, 1978) where convection was driven within the cell by thermal temperature gradients in the low Peclet number limit. A single eddy resulted. The magnetic field was concentrated into ropes adjacent to the vertical side walls when the magnetic Reynolds number was large, and the peak field $B^* \propto R^{1/2}B_0$, as Weiss (1966) had found for kinematic amplification of the field. The dynamic interaction in the fluid case necessarily required numerical solution. An analysis of the results showed the existence of kinematic, dynamic and magnetic drag regimes as for the rotating cylinder solution in § 3, with results for U, B^* and $\bar{B}$ very similar to figure 2. The functional dependencies in the three regimes were essentially the same as those given in (3.13), (3.14) and (3.15) although the constants of order unity were slightly different. The fluid convection problem and the rotating cylinder are similar configurations in that the flux number $\mathscr{H}$ is conserved, and that in the absence of the magnetic field the material would rotate roughly concentrically. The configurations also differ in a number of ways, namely (i) solid material versus fluid (ii) solid-body rotation versus viscous rotation law (iii) circle versus rectangle (iv) flux boundary condition applied on circular boundary versus flux boundary condition applied on horizontal boundary. Nevertheless the global behaviour is common, and this suggests that the similar features are more important than the differences.

One feature of the convective cell was the expulsion of the convective eddy from the side bands where the magnetic field is strong. This occurred when B^* was close to its maximum value B_m, and resulted in the reduction in the effective eddy size. This effect obviously cannot be present in the model of § 3. However, it is possible that it could be investigated with a cylinder model where the cylinder included an outer annulus which did not rotate, and the radius of the rotating part was variable.

For the rectangular fluid cell, $\bar{B}^2 = B_0\tilde{B}$ where $\tilde{B}$ is the average field on a vertical side wall. If the rectangle is of aspect ratio λ then $\mathscr{P} = B^*(1+\lambda)/\tilde{B}$. Examination of the numerical results showed $\mathscr{P}$ to be in the range 2 to 4—similar to the cylinder values.

The similarity in global behaviour between the rotating cylinder of § 3 and the fluid cell suggests that the solution for a cylinder rotating *in vacuo* in a vertical slot of the same diameter between two vertical perfectly insulating walls (thus ensuring constant $\mathscr{H}$) would also share these global characteristics.

7. Conclusions

A cylinder rotating *in vacuo* has been compared with one through which the applied magnetic flux is compelled to pass. When the field is sufficiently strong to permeate the cylinders—in the magnetic drag regime—the behaviour is similar. When the field is sufficiently weak—the kinematic regime—it is expelled from the central region of the cylinder and has negligible influence on the rotation rate. *In vacuo* much of the field is expelled completely; in the constant $\mathscr{H}$ case this is not possible—but the structure of the skin layer is identical. For sufficiently strong driving torques a third

intermediate regime occurs. For constant $\mathcal{H}$ this is the 'dynamic' regime in which small increases in the applied magnetic field result in a large decrease in the rotation rate. *In vacuo*, the intermediate regime consists of an overlap between the kinematic branch and the magnetic drag branch. There then exists a forbidden range of rotation rates, with hysteresis, involving sudden large changes in the rotation rate as the applied field is varied.

The behaviour of the constant $\mathcal{H}$ cylinder system has many similarities with low Peclet number convection driven in a horizontal fluid layer permeated by a vertical magnetic field. Both the convective system and the two cylinder configurations satisfy the magnetic braking equations (6.1).

In the relationship $\mathcal{H}B^* = \mathcal{P}\bar{D}\bar{B}^2$, between the peak magnetic field B^* and the RMS field $\bar{B}$, it is shown that $\mathcal{P} > 1$, strictly, so that this provides an upper bound for $\bar{B}$. Nevertheless in the systems considered in this paper, $\mathcal{P}$ is shown only to vary between 2 and 4 for all rotation rates; thus to within a factor of order unity $\mathcal{H}B^* \simeq \bar{D}\bar{B}^2$.

Acknowledgments

I am grateful to Dr R Hide for drawing my attention to the importance of the magnetic flux number and to the following for useful discussions: Drs M K Bevir, C G Gimblett, M R E Proctor and N O Weiss. P S Jackson and J Revie have provided computational assistance.

Appendix

The complex function $S(R)$ is defined by

$$S \equiv qJ_0(q)/J_1(q)$$

where $q^2 = -iR$ in which R is the magnetic Reynolds number, and so is proportional to the rotation rate of the cylinder. Figure 2 shows $\mathrm{Re}(S)$ and $\mathrm{Im}(S)$ as functions of R.

For small R (less than about 5)

$$\mathrm{Re}(S) \simeq 2 + 0.01R^2 \qquad \mathrm{Im}(S) \simeq \tfrac{1}{4}R.$$

For large R (greater than about 10)

$$\mathrm{Re}(S) \simeq \tfrac{1}{2} + (\tfrac{1}{2}R)^{1/2} \qquad \mathrm{Im}(S) \simeq (\tfrac{1}{2}R)^{1/2}.$$

If we write $S = \sigma \exp(i\phi)$ then

$$\sigma^2 = (\mathrm{Re}(S))^2 + (\mathrm{Im}(S))^2$$

and

$$\sigma \simeq \begin{cases} 2 + 0.025R^2 & \text{when } R \text{ small} \\ R^{1/2} & \text{when } R \to \infty. \end{cases}$$

The inverse function S^{-1} can be written in the forms

$$S^{-1} \equiv -J_0'(q)/qJ_0(q) = -\mathrm{d}(\ln J_0(q))/\mathrm{d}(q^2) = -i(\mathrm{d}/\mathrm{d}R) \ln (\mathrm{ber}\, R^{1/2} + i\, \mathrm{bei}\, R^{1/2})$$

where ber and bei are the Kelvin functions (Relton 1965). For small R

$$\mathrm{Re}(S^{-1}) \simeq 0.5 - 0.01\,R^2 \qquad \mathrm{Im}(S^{-1}) \simeq -R/16$$

and for large R

$$\mathrm{Re}(S^{-1}) \simeq (2R)^{-1/2} \simeq -\mathrm{Im}(S^{-1}).$$

It is also convenient to define

$$S - 1 \equiv \Sigma \exp(\mathrm{i}\beta);$$

then

$$\sigma \cos\phi = 1 + \Sigma \cos\beta \qquad \sigma \sin\phi = \Sigma \sin\beta$$

$$\Sigma \simeq \begin{cases} 1 + 0.04R^2 & \text{when } R \text{ small} \\ R^{1/2} & \text{when } R \to \infty \end{cases}$$

$$\beta \simeq \begin{cases} \frac{1}{4}R & \text{when } R \text{ is small} \\ \frac{1}{4}\pi + (8R)^{-1/2} & \text{when } R \to \infty \end{cases}$$

(see figure 5).

References

Gimblett C G and Peckover R S 1979 *Proc. R. Soc.* A **368** 75–97

Hide R 1978 *Nature* **271** 640–1

—— 1979 *Geophys. Astrophys. Fluid Dynamics* **12** 171–6

Moffatt H K 1978 *Magnetic Field Generation in Electrically Conducting Fluids* (Cambridge: Cambridge University Press) pp 53–62

Parker R L 1966 *Proc. R. Soc.* A **291** 60

Peckover R S and Gimblett C G 1981 *Bull. I.M.A.* **17** 73–8

Peckover R S and Weiss N O 1972 *Comput. Phys. Commun.* **4** 339–44

—— 1978 *Mon. Not. R. Astron. Soc.* **182** 189–208

Prandtl L and Tietjens O G 1974 *Applied Hydro- and Aeromechanics* (New York: Dover) p 43

Relton F E 1965 *Applied Bessel Functions* (New York: Dover)

Thom R 1975 *Structural Stability and Morphogenesis* (New York: Benjamin)

Weiss N O 1964 *Phil. Trans. R. Soc.* A **256** 99

—— 1966 *Proc. R. Soc.* A **293** 310–28